Scramjet Integration on Hypersonic Research Airplane Concepts

J. P. Weidner,* W. J. Small,† and J. A. Penland‡
NASA Langley Research Center, Hampton, Va.

Several rocket-boosted research airplane concepts were evaluated with a research scramjet engine to determine their potential to provide research on critical aspects of airframe-integrated hypersonic systems. Extensive calculations to determine the force and moment contributions of the scramjet inlet, combustor, nozzle, and airframe were conducted to evaluate the overall performance of the combined engine/airframe system at hypersonic speeds. Results of both wind-tunnel tests and analysis indicate that it is possible to develop a research airplane configuration that will cruise at hypersonic speed on scramjet power alone and also will have acceptable low-speed aerodynamic characteristics for landing.

Nomenclature

A_I = inlet capture area
A_c = inlet cowl area
Ar = reference area = 607 ft^2
C_D = drag coefficient, drag/qAr
C_L = lift coefficient, lift/qAr
C_m = pitching-moment coefficient, moment/$qAr\,L$
C_T = thrust coefficient, T/qAr
D = vehicle drag in flight direction
L = fuselage length, used as reference
L/D = lift-drag ratio, C_L/C_D
M = freestream Mach number
P = pressure
q = freestream dynamic pressure
R_L = freestream Reynolds number based on body length
T = scramjet engine thrust in flight direction
α = vehicle angle of attack, deg
ϕ = stoichiometric fuel to air equivalence ratio
θ_N = afterbody angle relative to forebody, deg
δ_e = elevon trim deflection, deg, positive for trailing edge down

Subscripts

t = trim condition, $C_m = 0$
base = denotes condition due to base area
∞ = freestream

Introduction

ONE key to sustained hypersonic flight is an efficient airbreathing hydrogen-fueled engine. Present research at NASA on airbreathing engine systems has focused on a fixed-geometry modularized scramjet concept that is integrated closely with the basic airframe of the hypersonic vehicle. The integrated scramjet engine/airframe, illustrated in Fig. 1, has been identified for a number of potential applications related to military, commercial, and space systems in the Mach 5 to 12 speed range. The hypersonic propulsion system typically consists of multiple engine modules attached to a forebody precompression surface and exhausting over a vehicle aftbody-nozzle surface. The inlets of multiple rectangular scramjet modules efficiently capture precompressed airflow contained between the vehicle and the forebody shock wave. The aftbody nozzle serves to increase scramjet nozzle expansion area and allows the external scramjet nacelle to be nearly stream aligned at the design Mach number for maximum installed thrust performance.

As a result of the asymmetrical forces on the aftbody nozzle, potentially large moments can occur. Care must be taken in nozzle design and location of the scramjet on the vehicle to minimize adverse pitching moments and resulting trim forces. This paper presents an analysis of the integration of a fixed-geometry scramjet concept being developed at NASA Langley Research Center with hypersonic research airplane configurations currently under study. Force components from the engine and airframe are derived analytically at hypersonic speeds, and the resulting overall performance in terms of thrust-to-drag ratio and vehicle trim is assessed. Modifications to the research airplane configurations, as well as modification to the scramjet-aftbody nozzle, are considered. Subsonic wind-tunnel data are used to examine approach and landing performance of the vehicle configurations with and without scramjet modules installed.

Engine Airframe Component Forces

A primary concern of any engine/airframe analysis is to account properly for all forces acting on the integrated vehicle. The components that are charged to engine or airframe systems vary from one study to another, depending on the bookkeeping procedure used. Figure 2 identifies the force-accounting procedure used in this study and separates the forces into two groups: net engine forces and net airframe forces. The scramjet concept described in Ref. 1 was selected as the engine concept for this study. This engine was designed to be integrated fully with a hypersonic airframe and features a fixed-geometry module that allows ingestion of the forebody boundary layer, eliminating a boundary-layer diverter between the engine module and vehicle. The forces illustrated in Fig. 2 and the methods in which they were derived are discussed in the following paragraphs.

Engine Forces

The net module thrust is defined as the difference between the momentum of the airflow entering the module and the momentum leaving the combustor exit. Net module force predictions are based on scramjet component efficiencies from wind-tunnel tests and analysis described, in part, in Refs. 2 and 3. Inlet spillage forces were derived from the wind-tunnel tests described in Ref. 3. External forces on the cowl were calculated using tangent wedge theory. Nozzle forces were derived analytically using a two-dimensional

Presented as Paper 76-755 at the AIAA/SAE 12th Propulsion Conference, Palo Alto, Calif., July 26-29, 1976; submitted Aug. 31, 1976; revision received Jan. 5, 1977.
Index categories: Aerodynamics; Airbreathing Propulsion.
*Aerospace Technologist.
†Aerospace Technologist. Member AIAA.

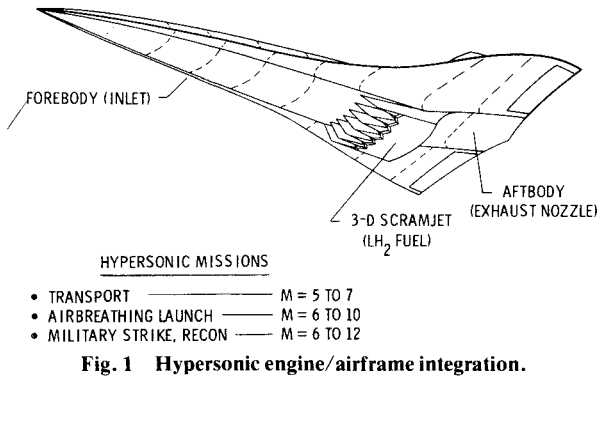

Fig. 1 Hypersonic engine/airframe integration.

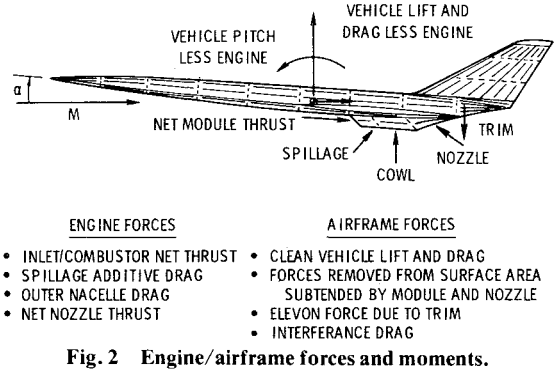

Fig. 2 Engine/airframe forces and moments.

finite-difference procedure that includes external/internal flow interactions.[4] A constant specific heat ratio was used to approximate frozen flow from the combustor exit through the nozzle.

Airframe Forces

The basic vehicle lift and drag and elevon trim forces were predicted using methods contained in Ref. 5. Surface areas covered by the engine module and nozzle are subtracted from the basic vehicle lift and drag when the engine is installed. Interference drag from corner flow and shock-wave interactions will result from module installation on the vehicle but have been neglected in this study.

Scramjet Nozzle Performance

The overall performance of the integrated scramjet is dependent upon mutual interactions that occur when the engine is combined with the vehicle undersurface. Figure 3 illustrates important aspects of these forces for a typical Mach 6 flight condition. The nozzle geometry illustrated in Fig. 3 was derived from the study reported in Ref. 6 and is considered the "reference" nozzle for this study. The nozzle has a planar top expansion surface at a 20° angle to the forebody. The cowl has a 6° internal expansion corner displaced 1.11 nozzle throat heights downstream from the upper 20° expansion corner. The total nozzle length is seven times the inlet cowl height (h_c). As can be seen from the pressure distribution shown in Fig. 3, the upper surface is near ambient pressure at the aft end of the nozzle, suggesting that little additional thrust would be obtained with further increases in nozzle length.

Thrust and moment coefficients from the combined module/nozzle also are shown in Fig. 3 as a function of nozzle length. As the nozzle length increases, the module is moved forward, affecting both thrust and pitching-moment coefficients produced by the engine. The reference nozzle produces over 50% of the total engine force, with the external portion of the nozzle contributing one-third of the nozzle force. Without the external nozzle, a positive nose-up pitching moment would be experienced.

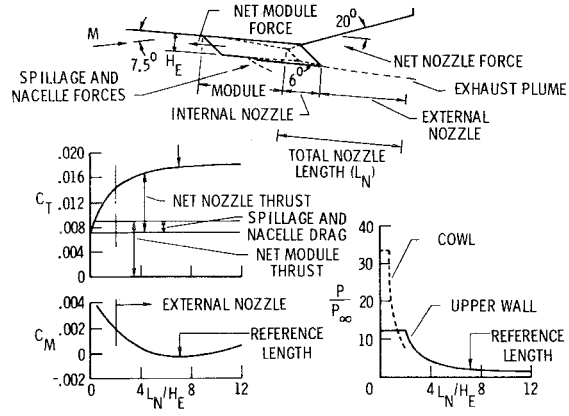

Fig. 3 Scramjet/nozzle performance at Mach 6, six 18-in. modules.

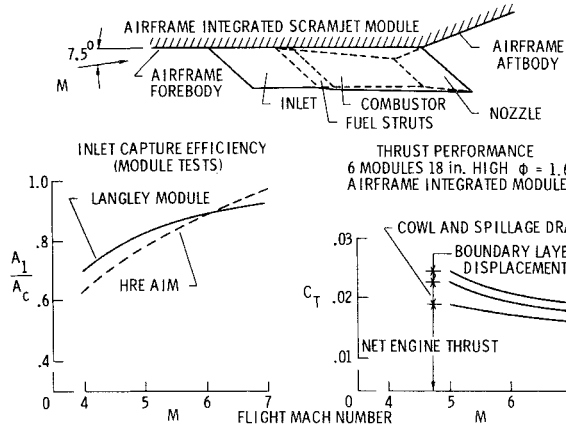

Fig. 4 Predicted scramjet performance.

The scramjet module inlet capture efficiency shown in Fig. 4 governs the quantity of airflow processed by the module and nozzle from which thrust is generated. The fixed-geometry scramjet inlet[3] has been tested from Mach 2 to Mach 6, exhibits self-starting characteristics throughout this speed range, and has a capture efficiency rivaling previous variable-geometry inlet concepts such as the HRE AIM inlet described in Ref. 7.

Engine thrust coefficient is shown in Fig. 4 over a Mach 5 to 7 speed range at a forebody precompression angle of 7.5° to the freestream airflow. The top curve is the net module and nozzle thrust, neglecting forebody boundary layer and outer nacelle drag forces. The effect of the boundary layer in displacing precompressed airflow along the forebody is estimated to result in an 8% to 10% loss in thrust due to mass loss through the engine. Performance is degraded further by the outer nacelle drag, particularly at lower Mach numbers, where the nacelle drag is increased by larger quantities of airflow spillage from the inlet.

Hypersonic Research Airplane

Integrated engine/airframe performance is tied closely to the combined vehicle/engine design, so that it is necessary to conduct studies with particular vehicle designs in mind. Results obtained through such studies can be expected to apply to other similar vehicles. The purpose of this paper is to combine the engine forces described in previous sections with airframe forces to assess resulting performance in terms of engine thrust relative to vehicle drag, and trim effects caused by the combined forces. The hypersonic research airplane configuration that evolved from a recent NASA/U.S. Air Force study is used as a focus for this integration analysis. The research airplane illustrated in Fig. 5 is defined as the "baseline concept" and is based on a set of criteria intended

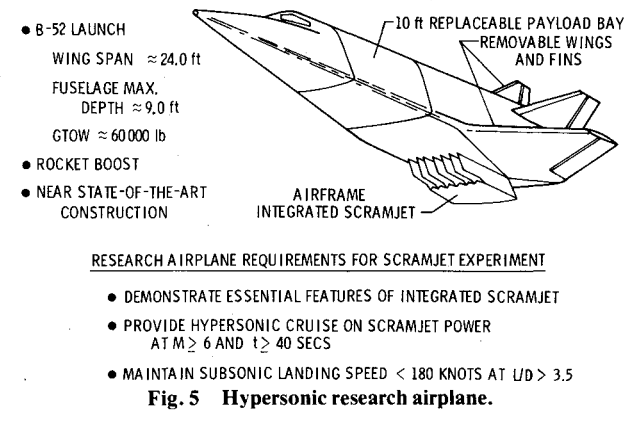

Fig. 5 Hypersonic research airplane.

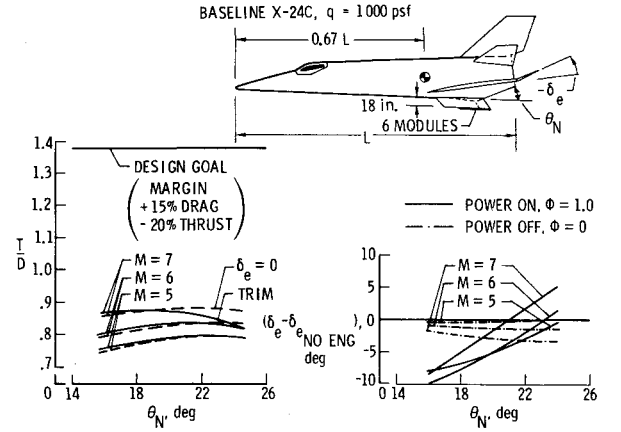

Fig. 6 Hypersonic engine/airframe integration on baseline X-24C at $q = 1000$ psf.

to provide a low-cost hypersonic test bed for aerodynamic, propulsion, and structure experiments. Primary requirements are a dedicated and replaceable payload bay section, removable wings and fins, and an unconstrained bottom surface for propulsion testing. The scramjet concept discussed in Ref. 1 could form a major experiment for this vehicle. The research airplane concept was developed to be air-launched from a B-52 aircraft and rocket-boosted to hypersonic speeds using existing rocket engines. The wing span, fuselage maximum depth, and gross takeoff weight listed in Fig. 5 were selected to conform to constraints imposed by the B-52 launch aircraft. Further details on this research airplane concept may be found in Ref. 8.

Current in-house research airplane studies include the baseline configuration derived from Ref. 8 and alternate configurations designed to improve aerodynamic performance. Initially, in this paper the baseline configuration performance is addressed at hypersonic speeds using both the analysis methods discussed previously and subsonic wind-tunnel data. Particular emphasis is directed to assessing the possibility of achieving steady-state cruise with the research airplane using thrust from a cruise scramjet experiment.

Performance of Baseline Concept

Engine integration studies of the baseline vehicle are being pursued in order to determine its compatibility with a cruise scramjet installation. For the purposes of this study, a propulsive package consisting of six 18-in.-high scramjet modules was used as a "standard" propulsive unit when comparing parametric design changes to the baseline vehicle and to other research aircraft concepts, which will be discussed later. The following sections discuss results of the hypersonic and subsonic investigation on the baseline research airplane configuration.

Hypersonic Performance

In determining the performance required to achieve equilibrium cruise on scramjet power, attention must be given to the expected normal decrement in performance which historically occurs between the time of conceptual design and the time of actual flight test. Scramjet developmental experience with the HRE[7] has shown a 20% thrust reduction from the initial planning stages of engine design to final test article. Similarly, a 15% increase in aerodynamic drag can be expected for this type of vehicle during its development cycle.[9] Accordingly, for this study, a thrust margin level of 1.38 times the analytically calculated value was considered necessary in order to insure cruise on scramjet power alone.

As identified in a previous analysis,[6] overall vehicle performance is sensitive to the scramjet module longitudinal location and therefore is considered in this study. Figure 6 shows the results of the analysis to determine optimum location for a vehicle weight at rocket burnout of approximately 24,000 lb at an altitude corresponding to a dynamic pressure of 1000 psf. Note from the figure that the nozzle trailing edge is fixed due to vehicle design constraints so that engine translation fore and aft changes the nozzle upper wall angle (θ_N). Changes in this nozzle wall angle affect the magnitude and location of the nozzle thrust vector. For a wide range of Mach numbers, a nozzle wall angle of 20° maximizes total vehicle thrust-to-drag levels. This corresponds to a lower cowl leading-edge position at 75% of the fuselage length. The sharp dropoff in trimmed thrust-to-drag ratio at Mach 7 for the aft engine location is due to a positive elevon deflection required to balance out large positive moment contributions from the nozzle.

For the speed range investigated in this study, thrust-to-drag ratios increased with Mach number. A primary cause of the thrust improvement is the reduced spillage and consequent improved inlet mass ingestion at higher speeds (see Fig. 4). At still higher Mach numbers, it is expected that thrust-to-drag levels will decrease with increasing Mach numbers as a result of decreasing scramjet combustor cycle efficiency.[6] Elevon trim changes also are presented in Fig. 6 as a difference in the deflection required to trim the vehicle with scramjets and without scramjets. The research airplane is intended to fly with or without a scramjet experiment, so that trim changes should be minimal between either configuration. Of importance also is the difference in elevon trim angles between scramjet power on ($\phi = 1$) and power off ($\phi = 0$). This vehicle must be controllable at hypersonic speeds during periods of engine stratup and shutdown. Therefore, small elevon trim changes are desired to minimize possible control problems. A poorly positioned engine such as the 16° nozzle case (Fig. 6) would require almost 10° of elevon movement between power-on and power-off conditions. For the baseline research aircraft concept, a nozzle wall angle near 20° results in a difference in δ_e of only 5°.

These results show that the "standard" six-module 18-in.-high scramjet cannot cruise the baseline concept. Even without the assumption of performance margins, this engine/airframe combination is unable to produce thrust equal to drag. To achieve cruise, either vehicle drag must be reduced and/or engine thrust must be increased. To obtain a better understanding of thrust and drag characteristics, a detailed component breakdown at Mach 6 is presented for the baseline vehicle and for engine forces through an angle-of-attack range (Fig. 7). Wave drag effects predominate vehicle drag levels and would be a major area for improvement through design modifications. Similarly, the large (66 ft^2) base area contributes about 15% of the total drag at cruise conditions ($\alpha = 5.8°$) and represents another area of potential improvement.

The engine/nozzle force breakdown shown on this figure represents the engine package and nozzle that would fit into the cutout area shown on the vehicle lower rear surface. Engine thrust is divided between net internal module and

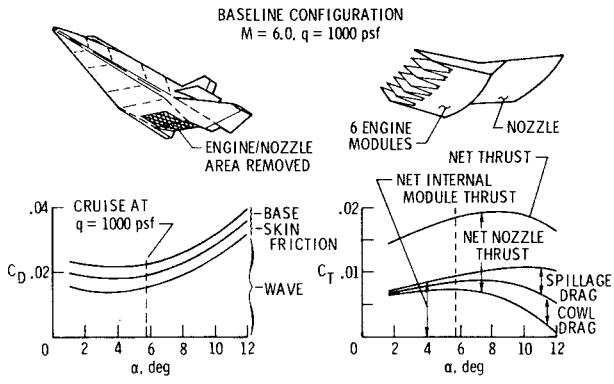

Fig. 7 Drag and thrust components.

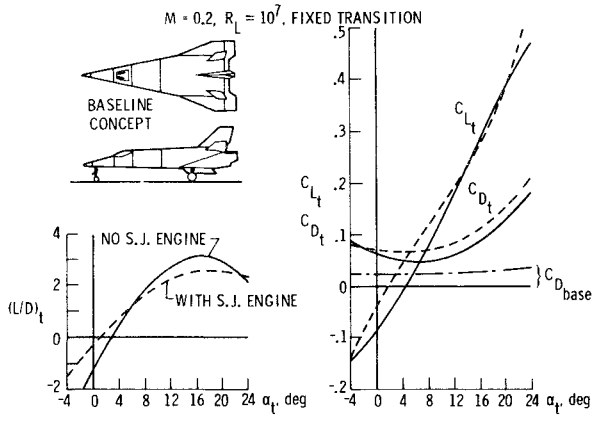

Fig. 8 Experimental subsonic performance, baseline concept; $M = 0.2, R_L = 10^7$, fixed transition.

nozzle forces for a large angle-of-attack range. Initially, total propulsion forces increase with angle of attack because of increased forebody compression and consequent increases in mass flow. At still higher angles of attack, local Mach numbers decrease, thus increasing inlet spillage and nacelle drag at a faster rate than thrust can be increased by forebody compression. A net thrust loss from the engine modules results. For this design concept, the ratios of thrust-to-drag curves maximize at angles of attack between about 4° and 7°, which correspond to equilibrium flight near $q = 1000$ psf.

Subsonic Performance

Wind-tunnel tests at $M = 0.2$ in the NASA Langley low-turbulence pressure tunnel were conducted on the baseline configuration with and without the standard six-module 18-in. scramjets. As shown in Fig. 8, trimmed $(L/D)_{max}$ was about 3.2 for the clean configuration and about 2.7 with the engine installed. A further loss of about 0.2 was incurred with simulated landing gears deployed. The large base drag is equal to one-half total C_{D_0} and is responsible for much of the poor subsonic performance. The addition of an engine package contributes another drag increment approximately equal in magnitude to the base drag. A low-speed $(L/D)_{max}$ of at least 3.5 (gear up) would be desirable for a manned research airplane. The poor landing performance of this configuration, particularly with the scramjet engine, is thus a source of concern. Although not discussed in this paper, the baseline concept exhibits poor-to-marginal longitudinal stability at hypersonic speeds. This low stability level and the previously discussed high- and low-speed performance problems have resulted in alternate configuration concepts being evaluated.

Performance of Alternate Configurations

Studies of the baseline configuration have suggested that improvements would be particularly useful in the areas of low- and high-speed drag and high-speed longitudinal stability. Thus, two configurations (Fig. 9) in addition to the baseline design have been investigated. Both alternate vehicle concepts contained the same propellant volume as the baseline concept and incorporated a 10-ft payload bay dedicated to experiments. The same body depth, wing span, and weight constraints imposed by the B-52 launch vehicle were applied to all concepts.

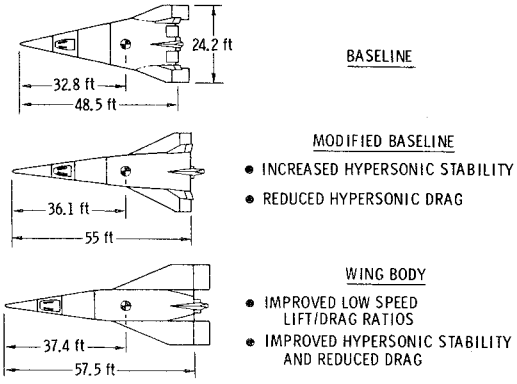

Fig. 9 Research airplane study configurations.

The first of these alternatives is a modified baseline concept with a higher fineness ratio fuselage which was intended to reduce hypersonic wave drag. Improved hypersonic longitudinal static stability as a result of reduced forward planform area was also a design goal. Base area, however, remained about the same as that of the baseline concept.

A second alternative (a wing-body concept) represents a more radical departure from the baseline vehicle. This design attempted to maximize subsonic performance by reducing base area and boattail drag to an absolute minimum. This led to a discrete high-fineness-ratio fuselage having a reduced forward plan area and a base area just large enough to enclose the boost rocket engine. A high-fineness-ratio fuselage reduced high-speed drag levels and improved hypersonic stability. Wing area also was increased to improve landing speeds with a cruise scramjet experiment.

Hypersonic Performance

Analytic studies of the cruise potential of these three vehicles on scramjet power alone were carried out at hypersonic speeds. Results for trimmed Mach 6 flight at a dynamic pressure of 1000 psf are shown in Fig. 10. Identical "standard" 18-in.-high, six-module scramjets were used on all vehicles. The analysis was conducted for a wide range of engine locations (nozzle wall angles) in order to see if the trend observed for the baseline in Fig. 6 was applicable to other design concepts. As presented in Fig. 10, the results show that a nozzle wall angle near 20° is near optimum for this class of vehicles, regardless of the details of design. Elevon deflections due to adding scramjets appear to be manageable for 20° nozzle wall angles. The degree of elevon deflection incurred by the addition of the engine either power-in or power-off is a function not only in engine location but also of elevon effectiveness. The wing-body concept had the highest elevon trim effectiveness of the three designs, which results in the rather minor changes shown for this vehicle.

Thrust-to-drag levels are improved noticeably for the modified configuration and increased still further with the wing-body configuration. This improvement is a direct result of the decrease in hypersonic drag attributable to the higher-fineness-ratio fuselages and, in the case of the wing body, a significant reduction in base area drag when compared to the baseline or modified concept. Although none of the vehicles were able to achieve the assumed thrust-to-drag margin with a "standard" scramjet, the wing-body configuration clearly needs less of an increase in engine size to achieve cruise than do the other two concepts.

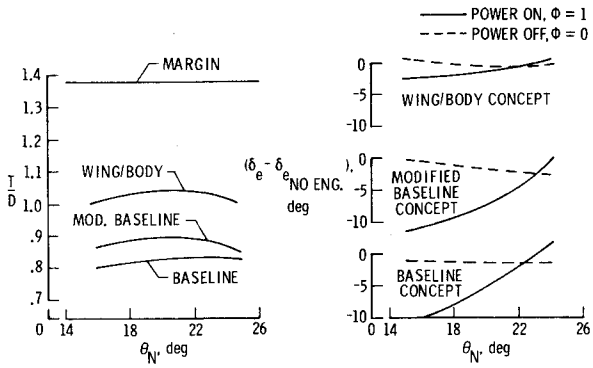

Fig. 10 Comparison of engine/airframe performance at Mach 6; $q = 1000$ psf, $C_L = 0.0376$, six modules, 18 in. high.

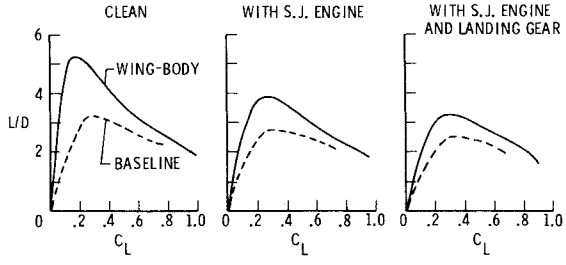

Fig. 11 Comparison of the experimental subsonic performance, baseline, and wing-body concepts; $M = 0.2$, $R_L = 10^7$.

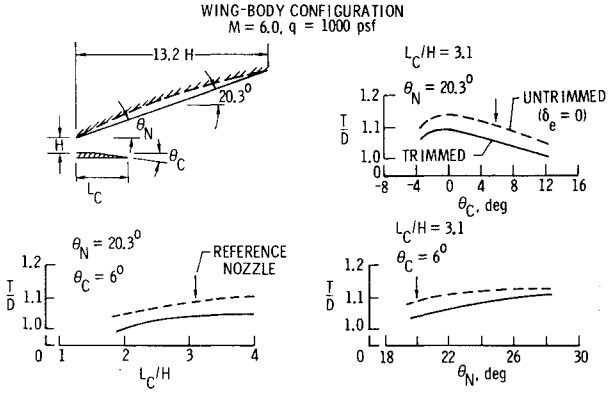

Fig. 12 Nozzle parametric evaluation.

Subsonic Performance

Subsonic wind-tunnel tests in the same facility used for the baseline concept were completed for the wing-body concept. A brief summary of the results is presented in Fig. 11. As compared to the baseline concept, the subsonic $(L/D)_{max}$ ratio greatly improved. The clean wing body has an $(L/D)_{max}$ of 5.2, which is 60% greater than the baseline. Installation of the scramjet six-module engine on the wing body resulted in an $(L/D)_{max}$ of 3.8, or about a 25% loss in $(L/D)_{max}$, and a further loss of about 15% was measured with the landing gear extended [$(L/D)_{max} = 3.3$]. Note that the goal of $(L/D)_{max}$ greater than 3.5 (gear up) was met at wind-tunnel Reynolds numbers out of ground effect. Furthermore, it may be anticipated that the value of $(L/D)_{max}$ of 3.3 with landing gear down is representative of the $(L/D)_{max}$ that may be expected at flight Reynolds numbers at trim during the roundout and touchdown phase of the landing maneuver.

Optimized Engine/Airframe Parameters

In the preceding discussion, deficiencies have been noted for the baseline design as a test bed for a cruise scramjet experiment at both high and low speeds. Of the modifications to the baseline considered to date, the wing-body concept has

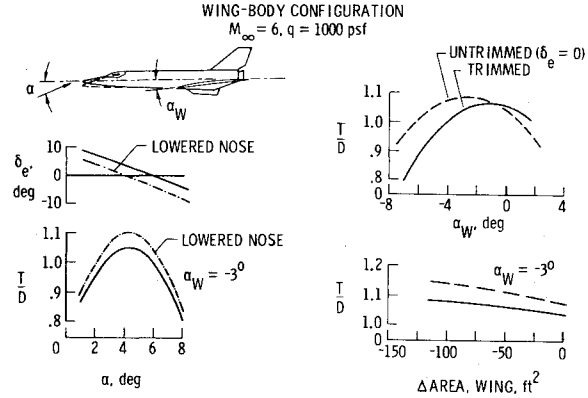

Fig. 13 Nozzle/airframe parametric evaluation.

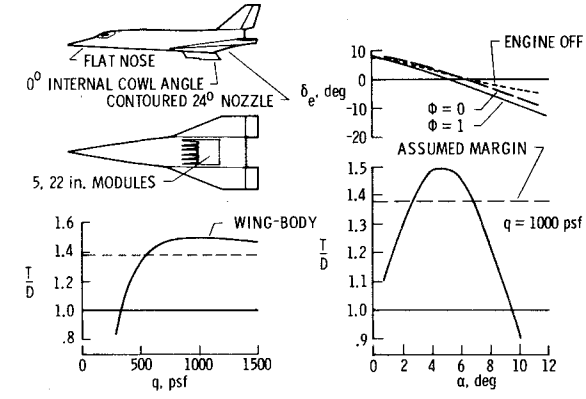

Fig. 14 Optimized wing-body configuration performance; $M_\infty = 6.0$.

shown the most overall promise as a potential carrier vehicle for research scramjets sizes to provide cruise thrust. Thus, the wing-body design was used as a standard from which additional scramjet/nozzle perturbations could be analyzed. The goal of this investigation was to determine the sensitivity of various airframe/engine/nozzle parameters on thrust efficiency. Many of the results from this analysis should be applicable to other research vehicle designs.

Figure 12 presents the results of a parametric study of nozzle geometric variables. For comparative purposes, all of the analyses were carried out with the standard six-module 18-in.-high scramjet. Note that, on Fig. 12, all trends are presented for trimmed and untrimmed ($\delta_e = 0°$) conditions. The untrimmed data are useful for identifying trends, since trim drag effect conceivably could be eliminated through vehicle modifications.

Thrust-to-drag sensitivity to lower wall cowl length was investigated first. Results showed that cowl extensions longer than the "reference" nozzle ($Lc/H = 3.1$) produced only 1% to 2% improvements in thrust. On the other hand, shortened cowl lengths appreciably reduced thrust levels. The final determination of proper cowl length also must account for the effect of cowl lengths on cowl weight and cooling requirements.

A second parametric study was made of lower cowl wall angle variation. As shown in Fig. 12, this angle (θ_c) was varied from a 12° expansion to a −3° compression. Changes in the lower cowl angle affect both interior lower cowl pressures and upper nozzle wall pressures. At 0° cowl angle, thrust in the flight direction was maximized. Additionally, the 0° cowl angle reduced external cowl drag from that of the "reference" nozzle. An additional benefit of reduced cowl angle is the improved ground clearance of the scramjet modules while the vehicle is attached to the B-52 launch aircraft.

Upper wall contour effects were studied briefly by deflecting an initial linear section of the upper nozzle wall and connecting this initial section to a fixed trailing-edge location with a parabolic curve (see Fig. 12). Increasing initial wall angle to about 24° increased thrust levels about 3%. Further wall angle increases improved thrust levels only slightly. As with other types of engine nozzles, contouring has a significant effect on reducing divergence losses.

As was noted in Fig. 7, the scramjet thrust and vehicle drag show a strong variation with angle of attack. It is possible, therefore, by adjusting the relative incidence of the wing to the fuselage, to investigate the effect of various trim angles of attack on thrust margin. Figure 13 shows that, indeed, wing incidence has a very strong influence on total vehicle thrust margin, with the original wing incidence of 2.9° producing the near-maximum thrust-to-drag values. For this vehicle, a 1° change in wing incidence produces a 0.24° change in trim angle of attack. Higher wing incidence angles lower the trim angle of attack and reduce thrust levels faster than drag is reduced. Lower wing incidence angles conversely increase trimmed vehicle angles of attack which increases drag at a greater rate than thrust increases. The displacement of the trimmed and untrimmed curves is primarily a consequence of the very large positive pitching moments that must be trimmed at the negative wing incidence angles.

Since at a cruise angle of attack at a dynamic pressure of 1000 psf the wing produces very little lift, a reduction in wing area might be expected to reduce wing drag and thus increase overall thrust-to-drag. Figure 13 shows that such effects are small for moderate decreases in wing area; therefore, wing area considerations will be dictated primarily by landing speed requirements rather than from an engine airframe integration criterion.

One possibility for reducing trim drag is shown in Fig. 13. The basic wing-body configuration has an upturned fuselage nose. Based on theoretical analysis, flattening the nose proved very effective in reducing pitching moments at the design angle of attack, consequently eliminating trim drag due to elevon deflection. Thrust-to-drag gains of 6% were realized by this technique. Other methods of reducing trim drag might prove equally effective; however, the method shown illustrates the point that aircraft trim with installed scramjets is an important design consideration early in vehicle development.

All previous calculations with the standard six-module 18-in.-high engine have fallen short of the minimum thrust-to-drag margin value of 1.38. By combining many of the improvements noted in Figs. 12 and 13 and increasing engine size 24% to a five-module, 22-in.-high propulsive package, it is possible to exceed this margin easily. Figure 14 shows the resulting thrust-to-drag developed by such an improved wing-body configuration. Excess performance above the margin allows this vehicle to cruise through a wide range of dynamic pressure levels. In particular, the lower dynamic pressures (near 500 psf) are typical of postulated hypersonic transport operating conditions. Flight into dynamic pressure regions above 1000 psf is limited by the thermal-structural design of the research airplane.

Performance Summary

A method of integration of a hypersonic scramjet engine to an airframe and a discussion of the sensitivity of overall engine performance to the various recognized design and integration parameters have been presented. An overview of the estimated flight performance of the baseline and the wing-body research airplane concepts is presented in Table 1. The landing $(L/D)_{max}$ is one measure of the subsonic aerodynamic efficiency and is presented in the table for the clean configurations, with scramjet engines attached, and with deployed tricycle landing gear. The $(L/D)_{max}$ values shown with an asterisk are from wind-tunnel tests of the standard 18-in.-high, six-module scramjet research engine system, and those values not marked with an asterisk are estimates for the larger engine required to cruise with the desired thrust-to-drag margin. This table illustrates the marked improvement in aerodynamic efficiency of the wing-body concept compared to the baseline vehicle.

Table 1 Performance summary with cruise scramjet

	Baseline		Wing-body	
Landing $(L/D)_{max}$				
Clean	3.15		5.22	
With scramjet engine	2.59	2.72[a]	3.75	3.84[a]
Landing gear and scramjet engine	2.44	2.52[a]	3.21	3.26[a]
Maximum boost Mach. no. (with LR-105)				
Clean	7.9		8.5	
With cruise scramjet engine	5.8		6.8	
Cruise capture area required, ft^2	16.68		12.45	

[a]Six-module, 18-in.-high scramjet.

From mission analyses based on experimental and calculated aerodynamics, the maximum boost Mach number utilizing the LR−105 rocket engine was determined for the three study concepts. Shown in Table 1 are peak boost Mach numbers for both the baseline and wing-body vehicles with and without the installed "standard" six-module cruise scramjet engine. The wing-body concept exhibits configuration design improvements across the speed range such that the clean vehicle maximum boost Mach number is increased by about 0.6 over the baseline concept, and the installed engine vehicle boost Mach number is 6.8 compared to 5.8. The large required inlet capture area shown in this table for the baseline concept increases the overall height of the vehicle, which complicates installation within the geometric constraints of the B-52 launch aircraft and may require a longer landing gear on the baseline aircraft. In addition, the added weight and drag of the larger engine contributes to the poor boost performance of the baseline concept. The smaller capture area requirement of the wing-body vehicle is a result of the lower hypersonic drag of that configuration.

It may be concluded that a low-drag vehicle such as the wing-body concept shows major performance benefits over a high-drag vehicle such as the baseline concept. Cruise scramjet requirements are eased, landing performance becomes acceptable, and rocket boost Mach number increases well into the hypersonic regime. Problem areas, of course, exist with all of the concepts studied; however, with proper design it appears possible to define a research airplane configuration capable of accepting a cruise scramjet experiment.

Conclusions

The possibility of defining an air-launched research airplane capable of cruising on a scramjet has been evaluated. Conclusions include the following:

1) Hypersonic cruise on scramjet power alone appears to be achievable on a research vehicle constrained to the size and weight requirements of a B-52 launch aircraft. Close attention must be paid to the vehicle and scramjet nozzle geometry to maximize scramjet thrust levels and minimize vehicle drag.

2) Acceptable subsonic performance can be achieved ($L/D>3.5$) with scramjet modules attached. This has been demonstrated in wind-tunnel tests on a wing-body configuration having a higher fineness ratio and smaller base area than the baseline concept.

3) Of the vehicles studied, the wing-body configuration had the highest subsonic L/D and the lowest hypersonic drag: a direct result of its smaller base area and higher-finesses-ratio fuselage.

4) With proper vehicle design, the elevon settings required for trim do not change significantly when a scramjet research experiment is added to the aircraft.

References

[1]Henry, J.R. and Anderson, G.Y., "Design Considerations for the Airframe-Integrated Scramjet," NASA TM X-2895, Dec. 1973.

[2]Anderson, G.Y., "An Examination of Injector/Combustor Design Effects on Scramjet Performance," presented at the *Second International Symposium on Air Breathing Engines,* Sheffield, England, March 25-29, 1974.

[3]Trexler, C.A., "Inlet Performance of the Integrated Langley Scramjet Module," presented at the *AIAA/SAE 11th Propulsion Conference,* Anaheim, Calif., Sept. 29-Oct. 1, 1975.

[4]Salas, M.D., "The Anatomy of Floating Shock Fitting," *AIAA Journal,* Vol. 14, May 1976, pp. 583-588.

[5]Gentry, A.E. and Smyth, D.N., "Hypersonic Arbitrary-Body Aerodynamic Computer Program (Mark III Version)," Douglas Aircraft Co., Rept. DAC61552 (Air Force Contracts F3361567C1008 and F3361567C1602), April 1968; Vol. I: "User's Manual," available from DDC as AD851811; Vol. II: "Program Formulation and Listings," available from DDC as AD815812.

[6]Small, W.J., Weidner, J.P., and Johnston, P.J., "Scramjet Nozzle Design and Analysis as Applied to a Highly Integrated Hypersonic Research Airplane," NASA TM X-71972, Nov. 1974.

[7]"Hypersonic Research Engine Project, Phase II – Aerothermodynamic Integration Model Development," Airesearch Manufacturing Co., Final Tech. Data Rept. AP-75-11133 (Contract NAS1-6666), May 19, 1975; available as NASA CR-132654.

[8]Kirkham, F.S., Jones, R.A., Buck, M.L., and Zima, W.P., "Joint USAF/NASA Hypersonic Research Aircraft Study," presented at the *AIAA Aircraft Systems and Technology Meeting,* Los Angeles, Calif., Aug. 4-8, 1975.

[9]Antonatos, P.P., Draper, A.C., and Neumann, R.D., AIAA Paper 70-1249, presented at the *AIAA Seventh Annual Meeting and Technical Display,* Houston, Texas, Oct. 19-22, 1970.